THE JOURNAL OF PHYSICAL CHEMISTRY B

Article

pubs.acs.org/JPCB

Photoinduced Changes of Surface Topography in Amorphous, Liquid-Crystalline, and Crystalline Films of Bent-Core Azobenzene-Containing Substance

Alexey Bobrovsky,[*,†] Konstantin Mochalov,[‡,§] Vladimir Oleinikov,[‡,§] Daria Solovyeva,[‡,§] Valery Shibaev,[†] Yulia Bogdanova,[†] Věra Hamplová,[∥] Miroslav Kašpar,[∥] and Alexej Bubnov[∥]

[†]Faculty of Chemistry, Moscow State University, Leninskie gory, Moscow, 119992 Russia

[‡]Laboratory of Biophysics, Shemyakin & Ovchinnikov Institute of Bioorganic Chemistry, Russian Academy of Sciences, 117871 Moscow, Russia

[§]Laboratory of Nano-Bioengineering, National Research Nuclear University "Moscow Engineering Physics Institute", 115409 Moscow, Russia

[∥]Institute of Physics, The Czech Academy of Sciences, 182 21 Prague 8, Czech Republic

Supporting Information

ABSTRACT: Recently, photofluidization and mass-transfer effects have gained substantial interest because of their unique abilities of photocontrolled manipulation with material structure and physicochemical properties. In this work, the surface topographies of amorphous, nematic, and crystalline films of an azobenzene-containing bent-core (banana-shaped) compound were studied using a special experimental setup combining polarizing optical microscopy and atomic force microscopy. Spin-coating or rapid cooling of the samples enabled the formation of glassy amorphous or nematic films of the substance. The effects of UV and visible-light irradiation on the surface roughness of the films were investigated. It was found that UV irradiation leads to the fast isothermal transition of nematic and crystalline phases into the isotropic phase. This effect is associated with *E*−*Z* photoisomerization of the compound accompanied by a decrease of the anisometry of the bent-core molecules. Focused polarized visible-light irradiation (457.9 nm) results in mass-transfer phenomena and induces the formation of so-called "craters" in amorphous and crystalline films of the substance. The observed photofluidization and mass-transfer processes allow glass-forming bent-core azobenzene-containing substances to be considered for the creation of promising materials with photocontrollable surface topographies. Such compounds are of principal importance for the solution of a broad range of problems related to the investigation of surface phenomena in colloid and physical chemistry, such as surface modification for chemical and catalytic reactions, predetermined morphology of surfaces and interfaces in soft matter, and chemical and biochemical sensing.

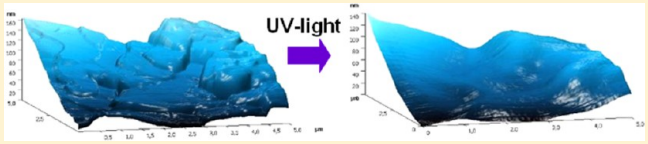

1. INTRODUCTION

Photofluidization and photoinduced mass-transfer processes occurring in polymer and low-molar-mass materials attract substantial attention because of their promising potential for applications in holography, optoelectronics,[1−7] different nano-devices, microlasers,[8] and so on. Most works related to these phenomena are focused on the process of surface-relief-grating (SRG) formation induced by the exposure of films of azobenzene-based low-molar-mass compounds or polymers with two interfering polarized laser beams.[9−17] Fewer works have dealt with photo-optical phenomena associated with the use of single-beam irradiation.[17−23] As was shown in a few studies, focused laser beam irradiation of amorphous azobenzene-based polymers induces directional mass transport and surface deformation along the polarization direction resulting in the formation of a hole (crater).[17−19] Recently,[20−23] the spontaneous formation of periodic surface relief under single-beam irradiation was observed and investigated. It was shown that, in some cases, the direction of the photoinduced gratings and material flow are strongly dependent on the direction of the incident light polarization.

In our recent works, the surface topography and optical properties of photochromic liquid-crystalline (LC) glass-forming systems were studied using a novel and unique experimental method combining polarizing optical microscopy (POM) and atomic force microscopy (AFM).[24,25] It was shown that slowly cooled samples of mixtures of cholesteric cyclosiloxanes with 10 wt % of azobenzene-containing dopant are characterized by the existence of "valleys" having a spiral superstructure. On the contrary, the quenched films demonstrate a spiral "hill" structure. Irradiation of the cholesteric mixture films with a focused laser beam (532 nm) leads to the

Received: March 26, 2016
Revised: May 12, 2016
Published: May 13, 2016

DOI: 10.1021/acs.jpcb.6b03122
J. Phys. Chem. B 2016, 120, 5073−5082

Chart 1

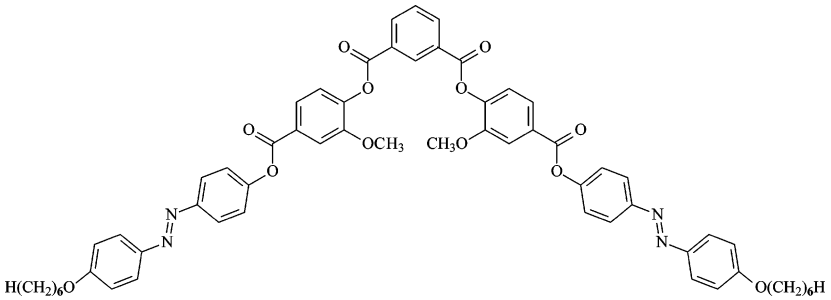

formation of partially aligned "hills" accompanied by a cooperative uniaxial orientation of chromophores and mesogenic groups in the direction perpendicular to the polarization plane of the incident light. The observed photo-optical effects were explained in terms of *E*−*Z* and *Z*−*E* isomerization cycles of azobenzene groups, anisotropic cooperative photoinduced rotational diffusion, and directional cooperative mass transport of chromophores and mesogens in the films.

More recently, photoinduced crater formation due to mass transfer outside the center of the beam in LC films containing high concentrations of azobenzene moieties was observed.[25] The depth of these craters is within the range of tens of nanometers and increases with the prolonging of the irradiation time. Attention is drawn to the fact that the rate of crater formation and the depth and diameter of the craters for nematic and cholesteric films are the same; in other words, the chirality of the systems has no substantial effect on the kinetics and the depth of the photoinduced craters. For uniaxially aligned films of nematic polymers, the mass transport proceeds only in the direction along the LC director. Such behavior is completely opposite to that observed for amorphous systems in which the mass transfer always occurs in the direction along the polarization plane.[17−19]

Among different types of photochromic compounds, bent-shaped compounds with azobenzene chromophore molecules are of special interest because of the combination of their unusual molecular architecture with functional photosensitivity.[26−35] To date, only two works have focused on photo-orientation processes in films of bent-shaped substances.[34,35] In a recent article, the photo-optical properties and photo-orientation processes in thin films of three novel bent-shaped azobenzene-containing compounds were studied.[35] It was demonstrated that UV-induced *E*−*Z* isomerization of azobenzene fragments is partially suppressed in crystalline films; nevertheless, these films are transformed from the crystalline to the amorphous state. Moreover, the action of polarized visible and UV light on thin films of bent-shaped azobenzene-containing compounds induces the photo-orientation of the chromophores in the direction perpendicular to the polarization plane. A high application potential was also demonstrated as the photoinduced isothermal melting and photo-orientation processes can respond to photo-optical data recording and storage demands.

On the other hand, the investigation of effects related to photofluidization and mass-transfer processes in bent-core photochromic compounds has still not been addressed. Thus, the present work is focused on a detailed study of photo-induced changes in the surface topography and crater formation processes in crystalline, liquid-crystalline, and amorphous films built up of a bent-shaped compound (denoted as **6WAVI**) with the specific chemical structure shown in Chart 1.

At room temperature, **6WAVI** is a crystalline powder with a melting point of 181 °C. At higher temperatures, the compound forms a nematic phase with a clearing point of 200 °C. This substance also exhibits other monotropic LC mesophases, which are not of specific interest for the present work.[35] The important point is that this specific compound can easily form amorphized films after spin-coating from chloroform solution. Such amorphous films are entirely stable at room temperature but can be easily transformed into a crystalline phase under annealing at 150 °C, far below the melting point.

The first part of this work is focused on the study of changes in the surface topography of crystalline and glassy nematic **6WAVI** films under UV irradiation; the second part describes the formation of craters in crystalline and amorphized films induced by localized focused blue-light irradiation (457.9 nm), and the third part details surface energy determinations based on contact angle measurements.

2. EXPERIMENTAL SECTION

2.1. Sample Preparation. The synthesis and characterization of the bent-shaped nonchiral **6WAVI** compound were described previously.[35] Thin films were prepared by the spin-coating method using a solution of the compound in chloroform at a concentration of 30 mg/mL. Thickness of the spin-coated films was measured by scanning AFM across scalpel scratches on one film; it was equal to ca. 110 nm.

2.2. Experimental Setup for Simultaneous AFM and POM Investigations. An advanced experimental setup, specifically designed for the purposes of this study, was used for simultaneous AFM and POM investigations combining the AFM scanning system, an upright optical microscope, an optical table for inverted optical microscopy, and cross-polarized illumination system (Scheme S1 in Supporting Information).

The samples (**1**) prepared as described above were placed directly on the top of scanning *XY*-piezostage (SmartSPM, AIST-NT) mounted into the *XY*-positioned table for inverted optical microscopy (**2**) with an open optical axis. The AFM head (**3**; SmartAFM, AIST-NT) was mounted onto the same optical table in a way that allowed the placement of AFM probe tip in the vicinity of a few micrometers to the optical axis. The spot of the blue laser (**4**, Ar^+ laser PLASMA LGN-519M), used for sample irradiation, was adjusted to the same spatial area using the deflectometer mirror of the AFM head, as shown in Scheme S1 (dashed box).

All optical images were obtained using an Optem Zoom 125C upright microscope (**5**) adjusted to the overall optical axis passed through the same point as the AFM probe tip.

DOI: 10.1021/acs.jpcb.6b03122
J. Phys. Chem. B 2016, 120, 5073−5082

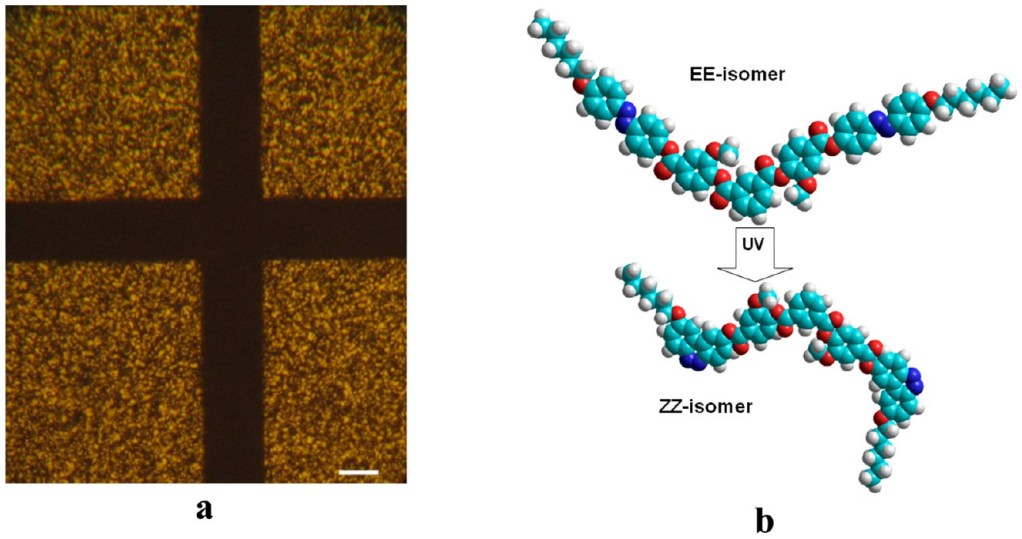

Figure 1. (a) POM image of an annealed crystalline film irradiated by UV light (380 nm, ~20 mW/cm^2) for 1 min through the mask. Dark areas correspond to the isotropic state. Scale bar = 50 μm. (b) Molecular models showing changes in **6WAVI** anisometry during UV irradiation.

The cross-polarized illumination system consisted of an ACE light source (**6**), a homemade condenser lens system (**7**), and a polymeric linear polarizing film (as a polarizer) (**8**) placed directly on the condenser at an arbitrary and fixed angle; a similar film used as the analyzer (**9**) was placed into a rotatable CCD/microscope coupler (**10**).

Angle of the analyzer film was adjusted by rotation of CCD/microscope coupler up to achieving of darkest field in POM image.

UV irradiation of the films was performed using a UV light-emitting diode (LED) (380 nm, ~20 mW/cm^2).

The average roughness was determined in a selected square area irradiated with LED. Roughness values were found as an integral profile of the selected area (standards: ASME B46.1-2009, ISO 4287-1997).

2.3. Contact Angle Measurements. Contact angle measurements were performed by the sessile drop technique. Advancing contact angles of probe liquids [water, ethylene glycol (EG), and diiodomethane (DIM)] at the **6WAVI** film surface were measured using a horizontal microscope equipped with a goniometer; the measurement accuracy was 1° at 20 °C. The dispersive and polar components of the surface energy for the **6WAVI** film were calculated by the two-liquid Owens–Wendt–Kaelble approach.[36] The determination of the surface energy components allows the intensity of intermolecular interactions in the film and its alteration as a result of external actions to be estimated.

3. RESULTS AND DISCUSSION

3.1. Changes in the Surface Topography of Crystalline and Nematic Films of 6WAVI under UV Irradiation. **6WAVI** films (prepared using the spin-coating method) were obtained in the form of a glassy state and completely isotropic because fast solvent evaporation prevents any ordering. Annealing of such films at 150 °C induces their crystallization, as was clearly observed by POM (Figure 1). The formation of crystallites was also revealed by AFM (Figure 2). Irradiation of such films with UV light induces a rapid transition to the isotropic state (dark areas in Figure 1a), which is associated with the E–Z isomerization of azobenzene chromophores accompanied by a decrease of molecular anisometry (Figure 1b). The occurrence of isomerization was confirmed by spectral measurements and appeared as a decrease of the absorbance peak corresponding to the π–π^* electronic transition of azobenzene chromophores taking place under UV irradiation (Figure S1).

The results of the AFM investigation of films irradiated for a short time (1 min) revealed that, even after complete isotropization, the films still had a rough surface resembling the initial crystalline surface topography (Figure 2). This effect is similar to the well-known paramorphism phenomenon peculiar for both crystal materials and liquid crystals.[37] After the occurrence of the phase transition, the morphology or texture of the sample did not change or resembles that of the initial phase. Nevertheless, prolonged UV irradiation resulted in a gradual smoothing of the surface, as seen in the AFM images (Figure 2), as well as the corresponding cross sections (Figure 3a).

This is a quite unexpected result that, to our knowledge, was observed for the first time in this work. UV irradiation induces fast disruption of three-dimensional positional crystalline order, whereas the photofluidization process requires a much longer time. For the studied compound having an extended bent-core aromatic fragment, the rate of photoinduced mass transfer at room temperature is very low, and under UV irradiation, the crystalline phase directly transforms into an amorphous solid film. As shown previously, amorphized spin-coated films of **6WAVI** exhibit a glass transition at temperatures higher than 100 °C.[35]

Figure 3b shows the changes in the calculated values of the surface roughness during the course of UV irradiation. The average roughness (R_q) decreased almost exponentially from 19.2 nm (before irradiation) to 5.6 nm (after 100 min of UV exposure).

Despite the dark Z–E isomerization, the irradiated films completely preserved the isotropic state and a smooth surface at room temperature because the glassy state of the films suppresses molecular mobility at temperatures below 100 °C. Nevertheless, annealing of the samples at 100–150 °C induced fast crystallization of the substance and the reappearance of the crystallites.

DOI: 10.1021/acs.jpcb.6b03122
J. Phys. Chem. B 2016, 120, 5073–5082

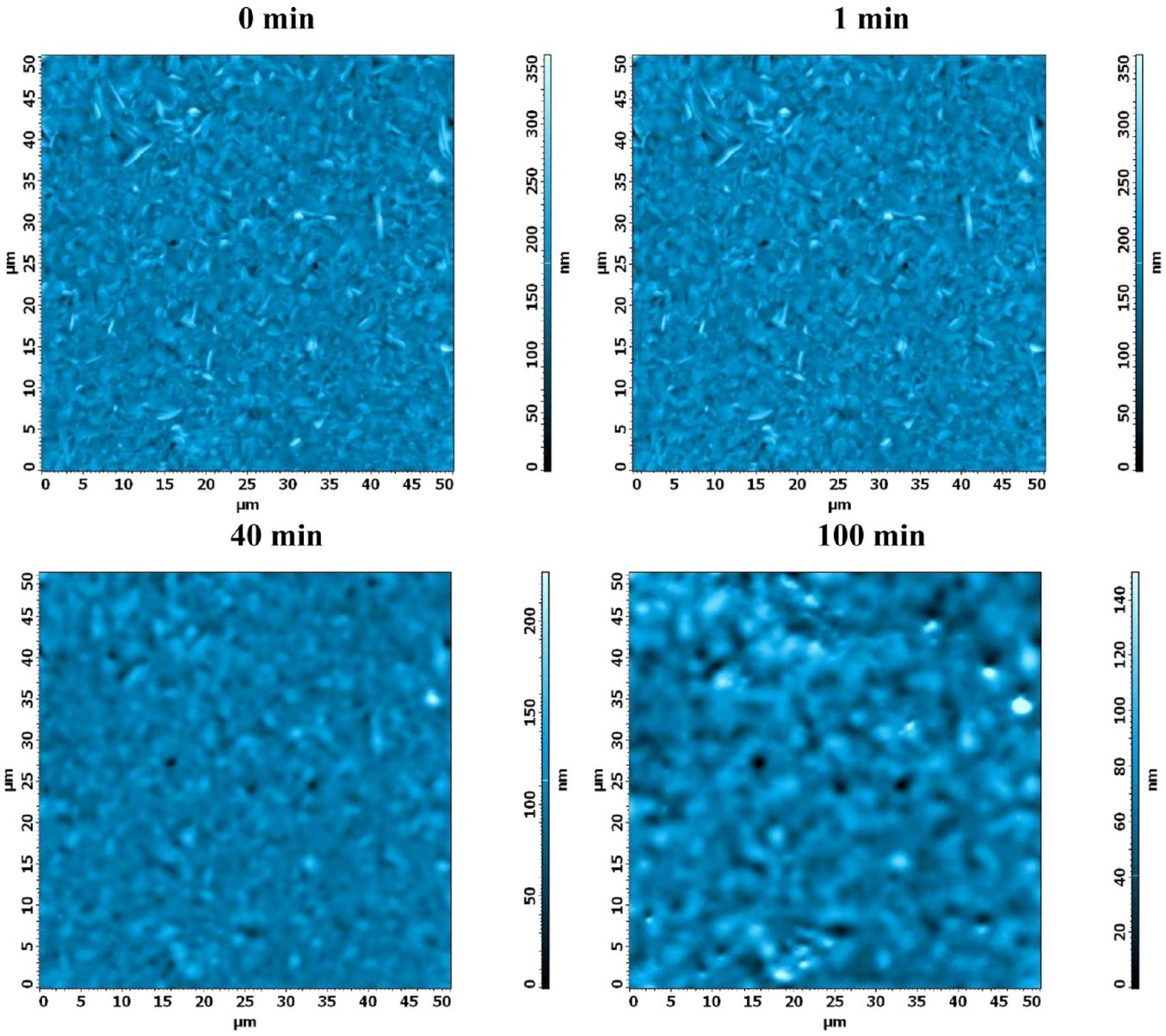

Figure 2. AFM images of an annealed crystalline film of **6WAVI** before and after UV irradiation (380 nm, ~20 mW/cm^2). Irradiation times are indicated in the figure.

To establish the effects of UV irradiation on the surface topography of **6WAVI** in both the crystalline and nematic phases, the spin-coated amorphized films were rapidly heated to ~190 °C and then quenched (rapidly cooled to room temperature by removing the sample from the hot stage). This method allows thin stable films to be obtained in which both the nematic and crystalline phases coexist (see the POM image in Figure 4). This method of sample preparation also enables larger crystallites of **6WAVI** to be obtained in comparison with those obtained upon annealing at 150 °C.

It is noteworthy that these phases are completely stable at room temperature and that the glassy state of the compound enables AFM imaging of the surface topographies of different phases to be performed (Figure 4).

The experimental setup used in our work allows one to find the exact correlation between the AFM and POM images of the films and compare the surface topographies of different phases: The nematic areas of the quenched films of **6WAVI** are characterized by higher roughness than the crystalline zones.

UV irradiation (1 min) induced the isotropization of both phases, which appeared as darkening of the POM images (Figure 4). At the same time, a slight smoothing of the surface topography occurred (Figure 4). The most noticeable changes in surface topography were observed under prolonged UV irradiation, for 10 and 40 min (Figures 4 and 5). A comparison of the photoinduced topography modifications of the crystalline and nematic phases is shown in Figure 5. From these observations, it can be concluded that more pronounced changes in the roughness of the surface occurred for the nematic phase (Figure 5b). Smoothing of the surface topography was accompanied by a significant deepening and widening of the cracks (Figure 4b–d) in zones corresponding to the crystalline phase.

Thus, UV irradiation enables the phase behavior of the films to be controlled, inducing fast film isothermal isotropization and promoting the process of decreasing the roughness of the surface topography. It is noteworthy that the smoothing process is much slower than the isothermal phase transition

DOI: 10.1021/acs.jpcb.6b03122
J. Phys. Chem. B 2016, 120, 5073−5082

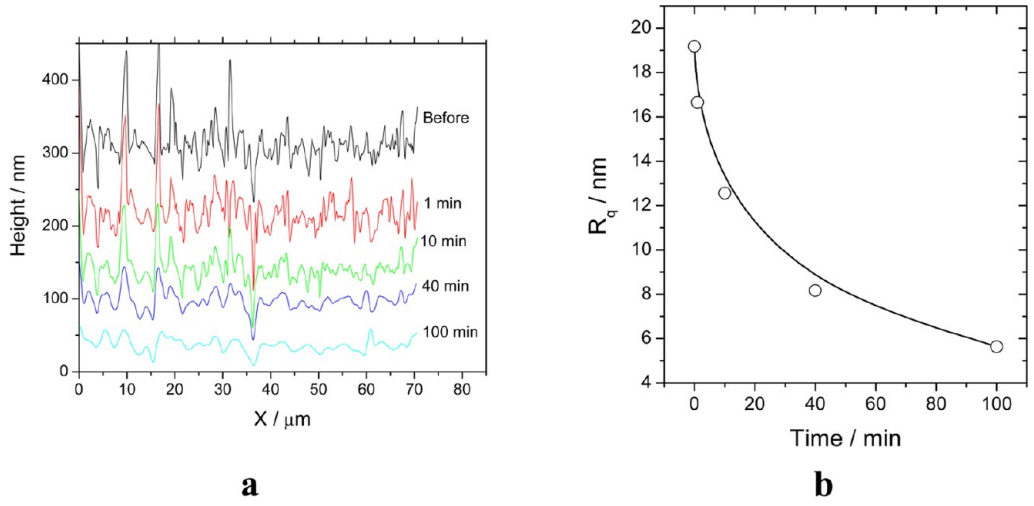

Figure 3. (a) Diagonal cross section and (b) average roughness values of the surface topography before and after UV irradiation of an annealed crystalline film of **6WAVI**. In panel a, curves are shifted relative to each other for clarity.

from the crystalline phase to the isotropic state, which can be explained by the low rate of mass-transfer processes in comparison with the rates of photoisomerization and isothermal melting of the crystalline phase. It should be pointed out that the effect of the photoinduced transition from the crystalline phase to the amorphous glassy state was observed in this work for the first time. Only a few previous works have investigated the photoinduced melting of an azobenzene-containing crystalline phase to the isotropic phase in the liquid aggregate state,[38,39] which is a rather different case than described in the present work.

3.2. Crater Formation in Crystalline and Amorphized Films of 6WAVI Induced by Localized Focused Blue Light Irradiation (457 nm). Irradiation of **6WAVI** films with unpolarized visible light (>450 nm) did not lead to any changes in the amorphous, nematic, or crystalline films. Probably, the absence of any noticeable photo-optical changes or surface topography modifications is associated with the very low concentration of *Z* isomer induced by a visible light: It is well-known that the irradiation of samples with visible light effectively induces back *Z*−*E* isomerization and produces mixtures of *E* and *Z* isomers with a low concentration of *Z* form.[40] The irradiation of amorphized films with polarized light of moderate intensity induces the photo-orientation of the azobenzene chromophores in the direction perpendicular to the polarization plane of the incident light. Recently, this photo-orientation phenomenon was studied in detail on films of this bent-core substance.[35]

In the present work, we have focused our attention on the effect of localized highly intensive polarized visible-light irradiation on the surface topography of amorphized and crystalline films of this bent-core compound. As the light source, a diode laser (457.9 nm) was used. The beam was focused in a Gaussian spot with a diameter of ca. 30 μm. Despite the low intensity of the beam (5 mW), its small diameter enabled a very high light power density to be achieved. Such localized focused laser irradiation was found to induce extreme mass transfer in amorphized and annealed crystalline **6WAVI** films (Figure 6). For amorphized films, laser irradiation with a duration of only 5 s induced clear crater formation (Figure 6a). Longer irradiation times increased the depth of the photo-optically induced craters (Figure 6b). The maximum values of the crater depth were almost equal to the thickness of the films; in other words, complete photoinduced dewetting of the films was observed.

It is necessary to mention that the effect of mass transfer was accompanied by the uniaxial alignment of chromophores. This can be clearly observed in the POM images of the irradiated film (Figure 6c,d) as the appearance of a noticeable birefringence in the irradiated spot. The appearance of two bright spots in the POM image can be explained by light scattering and propagation outside the irradiated area. The anisotropy of light scattering was clearly observed in the POM images and can be explained in terms of the dependence of the scattered light intensity on the direction of the incident beam polarization.

Irradiation with a green laser (532 nm) of similar intensity did not considerably affect the film topography because of the quite low absorbance of the compound in the green spectral region.

The direction of the observed mass transfer was found to be polarization-sensitive; that is, molecular transport occurred predominantly in a direction along the polarization plane (see 2D AFM images in Figure 6a,b), as well in cross sections of the craters parallel and perpendicular to the polarization plane of the laser beam (Figure S2).

Mass transfer occurred even in thin crystalline films (Figure S3), but the rate of the mass transfer was at least 1−2 orders of the magnitude lower than that observed in amorphous films.

For thick crystalline films, crater formation was much more prominent than for thin spin-coated films, and the depth of craters for thick films exceeded the range of 1 μm (Figures S4 and S5).

The observed crater formation could be explained by a strong gradient in the laser intensity of the focused beam. Azobenzene chromophores of **6WAVI** that are oriented predominantly along the polarization plane of the incident light (or, in other words, electric field vector) efficiently absorb light and undergo many cycles of *E*−*Z*−*E* photoisomerization. This photoisomerization process is accompanied by a rapid translational diffusional motion of **6WAVI** molecules. Because of the anisometry of the molecules, this motion occurs mostly in the direction along the long molecular axis. The probability and rate of the movement of the molecules is highest in the

DOI: 10.1021/acs.jpcb.6b03122
J. Phys. Chem. B 2016, 120, 5073−5082

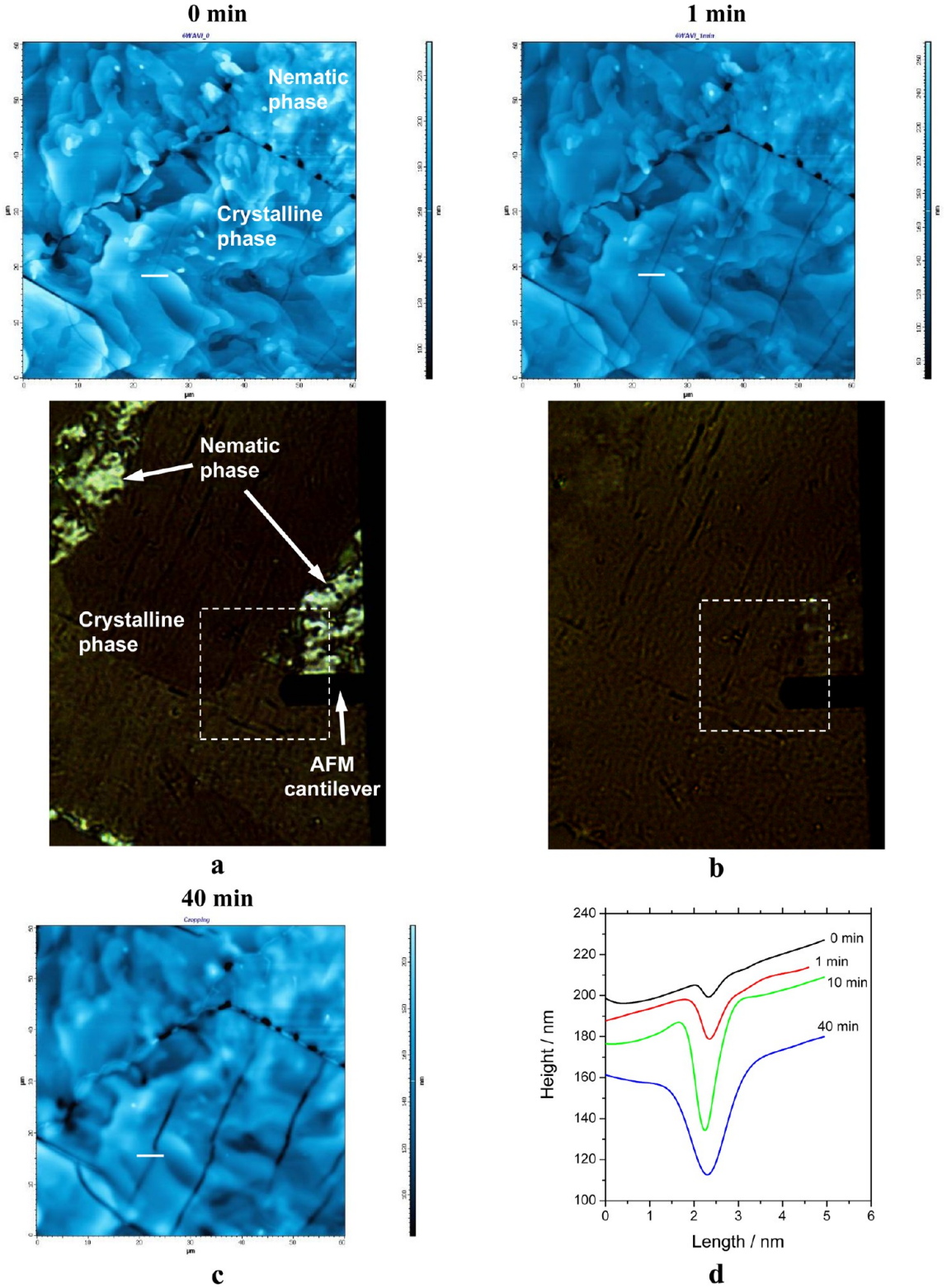

Figure 4. (a–c) AFM images of a quenched film of **6WAVI** before and after UV irradiation (380 nm, ~20 mW/cm^2). Irradiation times are shown in the figure. (a,b) POM microphotographs (see black color photographs) correspond to AFM images of the same film before (0 min) and after 1 min of irradiation. Corresponding AFM scan areas are shown by dashed white squares in the POM photographs. (d) Cross sections (shown by short white lines in the AFM scans in panels a–c), demonstrating the evolution of selected crack topographies under UV irradiation.

zones with the highest light intensity. Thus, eventually, the gradual flow of **6WAVI** molecules is realized in the direction opposite to the light intensity gradient, that is, outside the center of the laser beam. The polarization sensitivity of azobenzene chromophores results in a strong flow anisotropy that occurs in the direction along the polarization of the incident light.

DOI: 10.1021/acs.jpcb.6b03122
J. Phys. Chem. B 2016, 120, 5073–5082

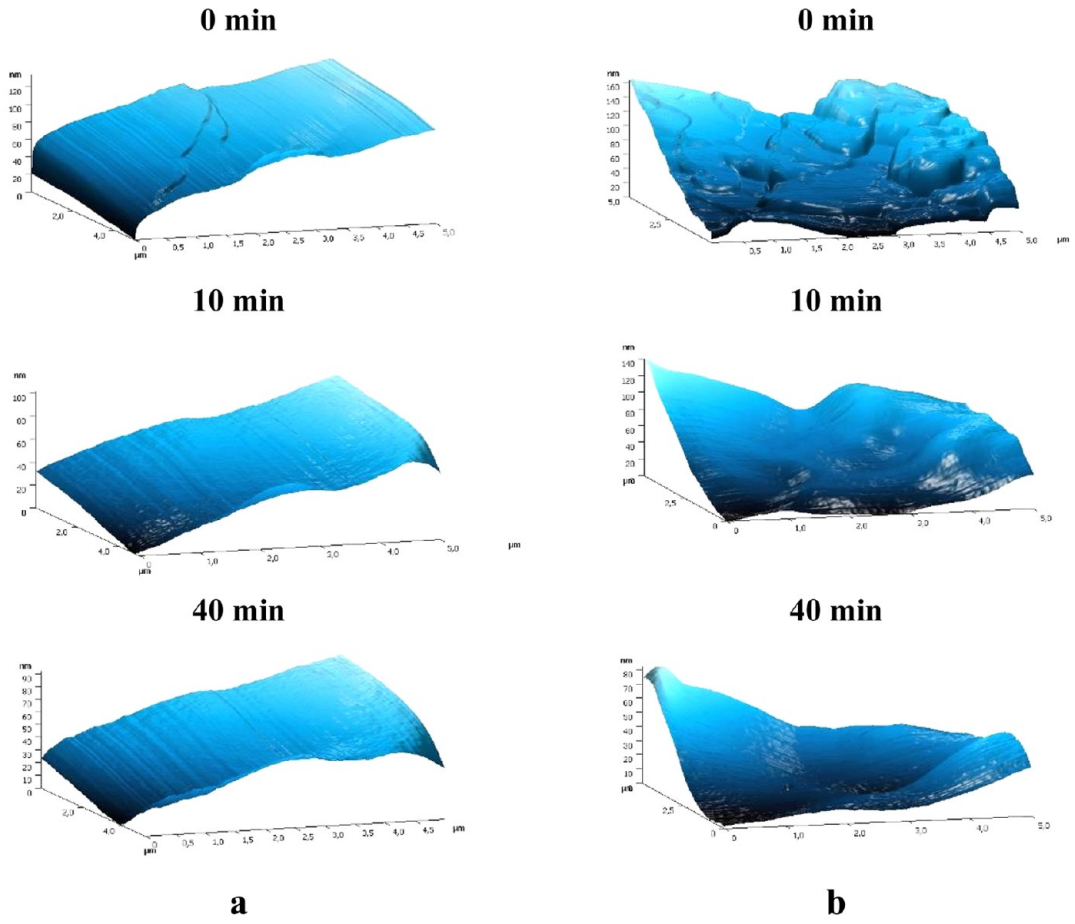

Figure 5. Changes in surface topography of (a) crystalline and (b) nematic zones of a quenched sample under UV irradiation.

It is very important to mention that there are two different types of photoinduced motion in **6WAVI** films subjected to polarized light irradiation. The first is related to the photo-orientation process described in detail recently.[35] In this case, azobenzene chromophores are photo-optically oriented in the direction perpendicular to the polarization plane of the incident light; that is, *rotational diffusion* is the most important effect underlying this phenomenon. On the other hand, the crater formation described in the present work is explained by another type of molecular motion, namely, *translational diffusion* of the chromophores.

Analysis of the obtained data and comparison with our previous results[25] reveals the principal difference between the "crater" formation process observed for LC polymers and for the specific bent-core compound described here. In LC polymers, the mass transfer is polarization-insensitive, and the direction of molecular flow is predetermined only by the initial alignment of the mesogenic groups in the LC films.

3.3. Effect of UV Irradiation on the Surface Free Energy. The initial surface of the **6WAVI** films was hydrophobic (Table 1). The water contact angles were close to those of other films of compounds containing azobenzene fragments in their structures.[41] It should be noted that, in general, θ_a values corresponding to the wetting of aromatic surfaces with water (84−86°)[42] should be expected to be the same as for azobenzene-containing compounds. However, this was observed only in the case of poly(azobenzene acrylate-*co*-fluorinated acrylate).[43] Values of water advancing contact angles at the film surfaces of most azobenzene derivatives with hydrocarbon or acyl substituents indicate the presence of methyl and methylene groups at the surface (104−96°).[41,44] For **6WAVI** films, drops of the test liquids were symmetrical and had good reproducibility at the different sites of the film surface. This fact points out the good energetic homogeneity of the surface.[45]

Values of the surface energy appeared to be invariant with respect to the probe liquid pairs [water/ethylene glycol (EG) and water/diiodmethane (DIM)]. The dispersive component of the **6WAVI** surface energy (γ_{SV}^{d}) made a major contribution to the total surface energy value (γ_{SV}): The polar components of the surface energy (γ_{SV}^{p}) appeared to be close to zero in all cases. This result is in a good agreement with previously obtained data.[41,43] Because the γ_{SV}^{d} value represents the intensity of dispersive (not polar) interactions between **6WAVI** molecules, which are not compensated at the film−gas interface, it is reasonable to suppose that the polar carbonyl groups in **6WAVI** film are oriented toward to glass substrate. The γ_{SV} value of **6WAVI** is close to 1, whereas for polyethylene, $\gamma_{SV} \approx 31$ mJ·m^{-2}.[46] Thus, the aromatic rings in the **6WAVI** film surface layer are screened by aliphatic groups from the probe liquids.

Despite the change in phase state, annealing did not much affect the contact angles of probe liquids and surface energy characteristics. This nontrivial, experimentally confirmed fact might be caused by the conservation of the orientations of the methyl and methylene groups of **6WAVI** and its packing density in the surface layer as a result of the phase transition.[47]

DOI: 10.1021/acs.jpcb.6b03122
J. Phys. Chem. B 2016, 120, 5073−5082

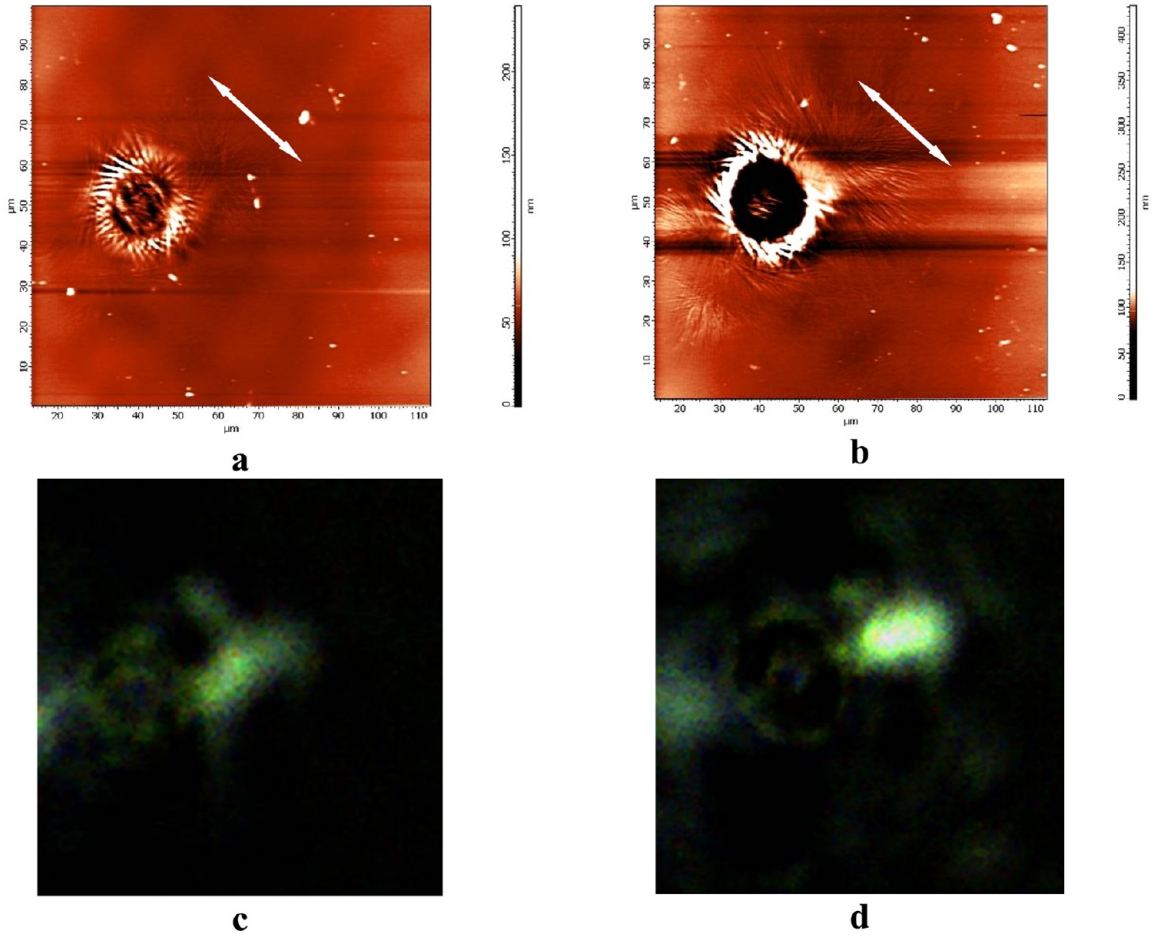

Figure 6. (a,b) AFM and (c,d) POM images of amorphized film of **6WAVI** after (a,c) 10 s and (b,d) 1 min of irradiation (457.9 nm, 5 mW). Arrows indicate the direction of laser polarization. The film was obtained by spin-coating and had a thickness of ~110 nm.

Table 1. Advancing Contact Angles of Probe Liquids at the Surface of a 6WAVI Film (θ_a) and Dispersive Component of the Surface Energy (γ_{SV}^d) under Various Conditions[a]

external conditions	θ_a (deg)			γ_{SV}^d (mJ·m^{-2})
	water	DIM	EG	
initial film	100	50	68	35
after annealing	100	49	72	36
after UV irradiation (1 h)	90	20	57	48
45 min after irradiation	98	48	70	36

[a]Errors in angle determinations and energy calculations are 1° and 1 mJ·m^{-2}, respectively. [b]$\gamma_{SV}^d = \gamma_{SV}$; γ_{SV}^p is close to zero for all conditions.

UV irradiation was found to lead to a reversible decrease of the contact angles of probe liquids (Table 1). This experimental fact is in good agreement with literature data related to the light-induced alteration of the wettability of azobenzene films.[41] After irradiation, the surface energy of the **6WAVI** films was closer to the polystyrene surface energy (42 mJ·m^{-2})[46] than to the polyethylene surface energy. The obtained data demonstrate the reorientation of **6WAVI** molecules in the surface layer of the film, which leads to an increase of γ_{SV}^d.

Earlier, a correlation was found between γ_{SV}^d and the gas permeability of polymer films, and a relationship between γ_{SV}^d and the fractional free volume of the polymer was demonstrated.[47] The clarification of the reasons for these correlations requires a separate theoretical study. The results of the surface energy calculations performed in this work and in refs 41 and 43 indicate the probable general character of the interrelation of the surface energy dispersive component and packing density of structural units of films of different substances in the surface layer.

4. CONCLUSIONS

For the first time, the surface topographies of amorphous, nematic, and crystalline films of an azobenzene-containing bent-core compound were investigated using a specifically designed experimental setup enabling the simultaneous application of two techniques, namely, polarizing optical microscopy and atomic force microscopy. It was found that *E*−*Z* photoisomerization of the compound under UV light induces a very fast transition from the crystalline or nematic phase to the isotropic state that is accompanied by a relatively slow smoothing of the surface. The rate of the latter process is much lower than the rates of the *E*−*Z* photoisomerization and isotropization processes. Localized irradiation by focused polarized visible light results in crater formation in amorphous and crystalline films. This process is polarization-sensitive, and mass transfer occurs predominantly in the direction along the polarization axis of the incident laser beam. Measurements of the contact angles of drops of different liquids on the film surface allowed for the determination of the surface energy and clearly demonstrated that the isomerization of **6WAVI** leads to a considerable increase in surface energy, which probably

DOI: 10.1021/acs.jpcb.6b03122
J. Phys. Chem. B 2016, 120, 5073−5082

occurs as a result of the reorientation of the molecules in the surface layer of the films.

■ ASSOCIATED CONTENT

Supporting Information

The Supporting Information is available free of charge on the ACS Publications website at DOI: 10.1021/acs.jpcb.6b03122.

Scheme of the experimental setup, absorbance spectra of a crystalline film of **6WAVI** before and after UV irradiation, and additional AFM data (PDF)

■ AUTHOR INFORMATION

Corresponding Author

*E-mail: bbrvsky@yahoo.com. Tel.: +7 495 939 11 89.

Notes

The authors declare no competing financial interest.

■ ACKNOWLEDGMENTS

This research was supported by the Russian Foundation of Fundamental Research (16-03-00455, 16-29-05140, study of UV-light-induced topography changes), the Russian Science Foundation [14-50-00131, investigations of crater formation by focused laser beam (A.B., V.S.); 14-03-00142, study of wetting behavior (Yu.B.)] and specific research projects of the Czech Science Foundation (16-12150S) and Ministry of Education, Youth and Sports of the Czech Republic (LH15305).

■ REFERENCES

(1) Lee, S.; Kang, H. S.; Park, J.-K. Directional Photofluidization Lithography: Micro/Nanostructural Evolution by Photofluidic Motions of Azobenzene Materials. *Adv. Mater.* **2012**, *24*, 2069−2103.

(2) Zhao, Y.; Ikeda, T. *Smart Light-Responsive Materials: Azobenzene-Containing Polymers and Liquid Crystals*; Wiley & Sons: Hoboken, NJ, 2009.

(3) Lefin, Ph.; Fiorini, C.; Nunzi, J.-M. Anisotropy of the photo-induced translation diffusion of azobenzene dyes in polymer matrices. *Pure Appl. Opt.* **1998**, *7*, 71−82.

(4) Nakano, H.; Suzuki, M. Photoinduced mass flow of photochromic molecular materials. *J. Mater. Chem.* **2012**, *22*, 3702−3704.

(5) Shibaev, V.; Bobrovsky, A.; Boiko, N. Photoactive liquid crystalline polymer systems with light-controllable structure and optical properties. *Prog. Polym. Sci.* **2003**, *28*, 729−836.

(6) Lee, S.; Kang, H. S.; Ambrosio, A.; Park, J.-K.; Marrucci, L. Directional Superficial Photofluidization for Deterministic Shaping of Complex 3D Architectures. *ACS Appl. Mater. Interfaces* **2015**, *7*, 8209−8217.

(7) Shibaev, V. P. Liquid-crystalline polymers: Past, present, and future. *Polym. Sci., Ser. A* **2009**, *51*, 1131−1193.

(8) Goldenberg, L. M.; Lisinetskii, V.; Gritsai, Y.; Stumpe, J.; Schrader, S. Single Step Optical Fabrication of a DFB Laser Device in Fluorescent Azobenzene-Containing Materials. *Adv. Mater.* **2012**, *24*, 3339−3343.

(9) Goldenberg, L. M.; Kulikovsky, L.; Kulikovska, O.; Tomczyk, J.; Stumpe, J. Thin Layers of Low Molecular Azobenzene Materials with Effective Light-Induced Mass Transport. *Langmuir* **2010**, *26*, 2214−2217.

(10) Fabbri, F.; Garrot, D.; Lahlil, K.; Boilot, J. P.; Lassailly, Y.; Peretti, J. Evidence of Two Distinct Mechanisms Driving Photo-induced Matter Motion in Thin Films Containing Azobenzene Derivatives. *J. Phys. Chem. B* **2011**, *115*, 1363−1367.

(11) Ikawa, T.; Kato, Y.; Yamada, T.; Shiozawa, M.; Narita, M.; Mouri, M.; Hoshino, F.; Watanabe, O.; Tawata, M.; Shimoyama, H. Virus-Templated Photoimprint on the Surface of an Azobenzene-Containing Polymer. *Langmuir* **2010**, *26*, 12673−12679.

(12) Vapaavuori, J.; Priimagi, A.; Kaivola, M. Photoinduced surface-relief gratings in films of supramolecular polymer−bisazobenzene complexes. *J. Mater. Chem.* **2010**, *20*, 5260−5264.

(13) Lee, S.; Shin, J.; Kang, H. S.; Lee, Y.-H.; Park, J.-K. Deterministic Nanotexturing by Directional Photofluidization Lithography. *Adv. Mater.* **2011**, *23*, 3244−3250.

(14) Saiz, L. M.; Ainchil, P.; Zucchi, I. A.; Oyanguren, P. A.; Galante, M. J. Surface Relief Gratings Inscription in Linear and Crosslinked Azo Modified Epoxy-Isocyanate Polymers. *J. Polym. Sci., Part B: Polym. Phys.* **2015**, *53*, 587−594.

(15) Lee, S.; Shin, J.; Lee, Y.-H.; Park, J.-K. Fabrication of the Funnel-Shaped Three-Dimensional Plasmonic Tip Arrays by Directional Photofluidization Lithography. *ACS Nano* **2010**, *4*, 7175−7184.

(16) Hurduc, N.; Donose, B. C.; Macovei, A.; Paius, C.; Ibanescu, C.; Scutaru, D.; Hamel, M.; Branza-Nichita, N.; Rocha, L. Direct observation of athermal photofluidisation in azo-polymer films. *Soft Matter* **2014**, *10*, 4640−4647.

(17) Bian, S.; Liu, W.; Williams, J.; Samuelson, L.; Kumar, J.; Tripathy, S. Photoinduced Surface Relief Grating on Amorphous Poly(4-phenylazophenol) Films. *Chem. Mater.* **2000**, *12*, 1585−1590.

(18) Bian, S.; Li, L.; Kumar, J.; Kim, D. Y.; Williams, J.; Tripathy, S. K. Single laser beam-induced surface deformation on azobenzene polymer films. *Appl. Phys. Lett.* **1998**, *73*, 1817−1819.

(19) Fiorini, C.; Prudhomme, N.; de Veyrac, G.; Maurin, I.; Raimond, P.; Nunzi, J.-M. Molecular migration mechanism for laser induced surface relief grating formation. *Synth. Met.* **2000**, *115*, 121−125.

(20) Ambrosio, A.; Girardo, S.; Camposeo, A.; Pisignano, D.; Maddalena, P. Controlling spontaneous surface structuring of azobenzene-containing polymers for large-scale nano-lithography of functional substrates. *Appl. Phys. Lett.* **2013**, *102*, 093102.

(21) Kandjani, S. A.; Barille, R.; Ortyl, E.; Dabos-Seignon, S.; Kucharski, S.; Nunzi, J.-M. Multistate addressing using one single beam polarization in an azobenzene polymer film. *Proc. SPIE* **2012**, *6259*, 62590T.

(22) Barille, R.; Ahmadi-Kandjani, S.; Ortyl, E.; Kucharski, S.; Nunzi, J.-M. Cognitive ability experiment with photosensitive organic molecular thin films. *Phys. Rev. Lett.* **2006**, *97*, 048701.

(23) Barille, R.; Nunzi, J.-M.; Ahmadi-Kandjani, S.; Ortyl, E.; Kucharski, S. One step inscription of surface relief microgratings. *Opt. Commun.* **2007**, *280*, 217−220.

(24) Bobrovsky, A.; Mochalov, K.; Chistyakov, A.; Oleinikov, V.; Shibaev, V. Features of double-spiral "valley-hills" surface topography formation in photochromic cholesteric oligomer-based films and their changes under polarized light action. *Macromol. Chem. Phys.* **2012**, *213*, 2639−2646.

(25) Bobrovsky, A.; Mochalov, K.; Chistyakov, A.; Oleinikov, V.; Shibaev, V. AFM study of laser-induced crater formation in films of azobenzene-containing photochromic nematic polymer and cholesteric mixture, J. *J. Photochem. Photobiol., A* **2014**, *275*, 30−36.

(26) Krishna Prasad, S.; Nair, G. G.; Sandhya, K. L.; Shankar Rao, D. S. Photoinduced Phase Transitions in Liquid Crystalline Systems. *Mol. Cryst. Liq. Cryst.* **2005**, *436*, 83−105.

(27) Rahman, L.; Kumar, S.; Tschierske, C.; Israel, G.; Ster, D.; Hegde, G. Synthesis and photoswitching properties of bent-shaped liquid crystals containing azobenzene Monomers. *Liq. Cryst.* **2009**, *36*, 397−407.

(28) Folcia, C. L.; Alonso, I.; Ortega, J.; Etxebarria, J.; Pintre, I.; Ros, M. B. Achiral Bent-Core Liquid Crystals with Azo and Azoxy Linkages: Structural and Nonlinear Optical Properties and Photoisomerization. *Chem. Mater.* **2006**, *18*, 4617−4626.

(29) Gimeno, N.; Pintre, I.; Martinez-Abadia, M.; Serrano, J. L.; Ros, M.B. Bent-core liquid crystal phases promoted by azo-containing molecules: from monomers to side-chain polymers. *RSC Adv.* **2014**, *4*, 19694−19702.

(30) Zep, A.; Sitkowska, K.; Pociecha, D.; Gorecka, E. Photo-responsive helical nanofilaments of B4 Phase. *J. Mater. Chem. C* **2014**, *2*, 2323−2327.

DOI: 10.1021/acs.jpcb.6b03122
J. Phys. Chem. B 2016, 120, 5073−5082

(31) Nair, G. G.; Prasad, S. K.; Hiremath, U. S.; Yelamaggad, C. V. Effect of light on the polarization of a banana-shaped achiral compound doped with a photoactive azobenzene material. *J. Appl. Phys.* **2001**, *90*, 48−52.
(32) Jákli, A.; Prasad, V.; Shankar Rao, D. S.; Liao, G.; Jánossy, I. Light-induced changes of optical and electrical properties in bent-core azo compounds. *Phys. Rev. E* **2005**, *71*, 021709.
(33) Alaasar, M.; Prehm, M.; Tschierske, C. Influence of halogen substituent on the mesomorphic properties of five-ring banana-shaped molecules with azobenzene wings. *Liq. Cryst.* **2013**, *40*, 656−668.
(34) Tamba, M.-G.; Bobrovsky, A.; Shibaev, V.; Pelzl, G.; Baumeister, U.; Weissflog, W. Photochromic azobenzene functionalized banana−calamitic dimers and trimers: mesophase behaviour and photo-orientational phenomena. *Liq. Cryst.* **2011**, *38*, 1531−1550.
(35) Bobrovsky, A.; Shibaev, V.; Hamplová, V.; Bubnov, A.; Novotná, V.; Kašpar, M.; Piryazev, A.; Anokhin, D.; Ivanov, D. Photo-optical properties of amorphous and crystalline films of azobenzene-containing photochromes with bent-shaped molecular structure. *J. Photochem. Photobiol., A* **2016**, *316*, 75−87.
(36) Kloubek, J. Development of methods for surface free energy determination using contact angles of liquids on solids. *Adv. Colloid Interface Sci.* **1992**, *38*, 99−142.
(37) *Liquid Crystals: Experimental Study of Physical Properties and Phase Transitions*; Kumar, S., Ed.; Cambridge University Press: Cambridge, U.K., 2011.
(38) Akiyama, H.; Kanazawa, S.; Okuyama, Y.; Yoshida, M.; Kihara, H.; Nagai, H.; Norikane, Y.; Azumi, R. Photochemically Reversible Liquefaction and Solidification of Multiazobenzene Sugar-Alcohol Derivatives and Application to Reworkable Adhesives. *ACS Appl. Mater. Interfaces* **2014**, *6*, 7933−7941.
(39) Okui, Y.; Han, M. Rational design of light-directed dynamic spheres. *Chem. Commun.* **2012**, *48*, 11763−11765.
(40) *Photochromism, Molecules, and Systems*, Dürr, H., Bouas-Laurent, H., Eds.; Elsevier: Amsterdam, 1990.
(41) Yang, D.; Piech, M.; Bell, N. S.; Gust, D.; Vail, S.; Garcia, A. A.; Schneider, J.; Park, C.-D.; Hayes, M. A.; Picraux, S. T. Photon Control of Liquid Motion on Reversibly Photoresponsive Surfaces. *Langmuir* **2007**, *23*, 10864−10872.
(42) Butt, H.-J.; Ecke, S.; Heim, L. O.; Heiskanen, K.; Preuss, M.; Raiteri, R.; Schreithofer, N.; Vinogradova, O. I.; Yakubov, G. E. Microsphere tensiometry to determine contact angles on individual particles. In *Contact Angle, Wettability and Adhesion*; Mittal, K., Ed.; VSP Publishers: Boston, 2002; Vol. *2*, pp 201−214.
(43) Abrakhi, S.; Peralta, S.; Fichet, O.; Teyssie, D.; Cantin, S. Poly(azobenzene acrylate-co-fluorinated acrylate) Spin-Coated Films: Influence of the Composition on the Photo-Controlled Wettability. *Langmuir* **2013**, *29*, 9499−9509.
(44) Pyter, R. A.; Zografi, G.; Mukerjee, P. Wetting of solids by Surface-Active Agents: The effects of unequal adsorption to vapor-liquid and solid-liquid interfaces. *J. Colloid Interface Sci.* **1982**, *89*, 144−153.
(45) De Gennes, P. G. Wetting: Statics and Dynamics. *Rev. Mod. Phys.* **1985**, *57*, 827−863.
(46) Lee, L. H. Correlation between Lewis-Acid-Base Surface Interaction Components and Linear Solvation Energy Relationship Solvatochromic α and β Parameters. *Langmuir* **1996**, *12*, 1681−1687.
(47) Bogdanova, Y. G.; Dolzhikova, V. D.; Filippov, A. N. Contact angles as indicators of macromolecule packing density at polymer surface. In *European Polymer Congress. Book of Abstracts*; European Polymer Federation: Strasbourg, France, 2013; pp 3−17.

DOI: 10.1021/acs.jpcb.6b03122
J. Phys. Chem. B 2016, 120, 5073−5082